Syncollin inhibits regulated corticotropin secretion from AtT-20 cells through a reduction in the secretory vesicle population

Barbara WÄSLE*, Lori B. HAYS†, Christopher J. RHODES† and J. Michael EDWARDSON*[1]

*Department of Pharmacology, University of Cambridge, Tennis Court Road, Cambridge CB2 1PD, U.K., and †Pacific Northwest Research Institute, 720 Broadway, Seattle, WA 98122, U.S.A.

Syncollin is a 13 kDa protein that is highly expressed in the exocrine pancreas. Syncollin normally exists as a doughnut-shaped homo-oligomer (quite probably a hexamer) in close association with the luminal surface of the zymogen granule membrane. In the present study, we examine the effect of expression of syncollin in AtT-20 neuroendocrine cells, which do not normally express this protein. Efficient expression was achieved by infection of the cells with adenoviral constructs encoding either untagged or GFP (green fluorescent protein)-tagged syncollin. Both forms of the protein were sorted into corticotropin (ACTH)-positive secretory vesicles present mainly at the tips of cell processes. Neither form affected basal corticotropin secretion or the constitutive secretion of exogenously expressed secreted alkaline phosphatase. In contrast, regulated secretion of corticotropin was inhibited (by 49 %) by untagged but not by GFP-tagged syncollin. In parallel, untagged syncollin caused a 46 % reduction in the number of secretory vesicles present at the tips of the cell processes. Syncollin–GFP was without effect. We could also show that native syncollin purified from rat pancreas was capable of permeabilizing erythrocytes. We suggest that syncollin may induce uncontrolled permeabilization of corticotropin-containing vesicles and subsequently destabilize them. Both forms of syncollin were tightly membrane-associated and appeared to exist as homooligomers. Hence, the lack of effect of syncollin–GFP on regulated exocytosis suggests that the GFP tag interferes in a subtler manner with the properties of the assembled protein.

Key words: AtT-20 cells, corticotropin, exocytosis, secretory vesicle, syncollin.

INTRODUCTION

Syncollin is a 13 kDa protein expressed in the exocrine pancreas, and was originally identified by its binding to the SNARE (soluble *N*-ethylmaleimide-sensitive fusion protein attachment protein receptor) syntaxin [1]. It has become clear that syncollin associates tightly with the luminal surface of the zymogen granule membrane [2], casting doubt on the physiological significance of its ability to bind to syntaxin. Syncollin is known to exist in the form of a doughnut-shaped homo-oligomer, most probably a hexamer [3], which interacts with membranes in a cholesterol-dependent manner [4]. It resists extraction from the granule membrane in high-salt buffer solutions, but is removed under alkaline conditions (pH > 10), when it becomes monomerized [2]. Syncollin associates with GP-2, the major glycoprotein present in the granule membrane [5]. Both proteins are associated with detergent-insoluble, cholesterol-enriched complexes, indicating that they are present in lipid 'rafts', which also contain the SNAREs syntaxin 3 and synaptobrevin 2 [5].

Although syncollin is now fairly well characterized biochemically, its physiological function is still unclear. In rats, the expression of syncollin is modulated by changes in feeding patterns [6], suggesting that it does play a role in the secretion of digestive enzymes. Surprisingly, secretion of digestive enzymes was normal in syncollin-deficient mice, although the acute pancreatitis observed in response to hyperstimulation was more severe than normal [7]. In an attempt to learn more about the cellular role of syncollin, we have overexpressed it in the AtT-20 neuroendocrine cell line, which secretes corticotropin (ACTH) in response to increases in cAMP levels. We show that syncollin [both untagged and tagged at its C-terminus with GFP (green fluorescent protein)] is targeted to secretory vesicles in AtT-20 cells. Neither form of syncollin affects the basal secretion of corticotropin or the constitutive release of SEAP (secreted alkaline phosphatase) from the cells. In contrast, syncollin, but not syncollin–GFP, significantly reduces both the regulated secretion of corticotropin and the number of large, dense-core secretory vesicles at the tips of the cell processes. Possible mechanisms that may underlie this effect of syncollin are discussed.

EXPERIMENTAL

Adenoviral constructs

Recombinant adenoviruses expressing syncollin, syncollin–GFP, GFP and SEAP were generated, amplified and purified as described previously [8–10]. Adenoviruses were stored in 20 % (v/v) glycerol at − 80 °C.

Cell culture and infection

AtT-20 cells were grown in DMEM (Dulbecco's modified Eagle's medium), containing 10 % (v/v) foetal bovine serum, 100 units/ml penicillin, 100 mg/ml streptomycin and 2 mM L-glutamine in an atmosphere of 5 % CO_2/air. For adenoviral infection, fresh medium containing (4–12) × 10^9 plaque-forming units/ml of virus

Abbreviations used: 8-Br-cAMP, 8-bromo-cAMP; BS^3, bis(sulphosuccinimidyl)suberate; DMEM, Dulbecco's modified Eagle's medium; GFP, green fluorescent protein; HBS, Hepes-buffered saline; HRP, horseradish peroxidase; MβCD, methyl-β-cyclodextrin; SEAP, secreted alkaline phosphatase; SNAP-25, synaptosome-associated protein of 25 kDa; SNARE, soluble *N*-ethylmaleimide-sensitive fusion protein attachment protein receptor; TRITC, tetramethylrhodamine isothiocyanate.

[1] To whom correspondence should be addressed (e-mail jme1000@cam.ac.uk).

was added to the cells. After a 2 h incubation at 37 °C, the cells were washed with virus-free medium and then maintained in fresh medium for at least 16 h to allow protein expression.

Gel electrophoresis and immunoblotting

Proteins were separated by SDS/PAGE and then electrophoretically transferred on to nitrocellulose (Schleicher and Schuell) by semi-dry blotting. Blots were probed with primary antibodies at dilutions of 1:500–1:1000. Immunoreactive bands were visualized using HRP (horseradish peroxidase)-conjugated secondary antibodies (1:1000) and SuperSignal (Pierce and Warriner).

Immunocytochemistry and confocal microscopy

Immunocytochemistry on AtT-20 cells growing on poly(D-lysine)-coated (1 mg/ml) glass coverslips was performed as described previously [11]. Cells were visualized with a Leica NT-TCS confocal laser-scanning microscope, using a × 100 objective lens with a 1.0 numeric aperture. Images were collected with appropriate filters: GFP and FITC were excited using the 488 nm line of a krypton/argon laser and imaged with a 510–540 nm band-pass filter. Cy3 and TRITC (tetramethylrhodamine isothiocyanate) were excited with the 568 nm line and imaged with a long-pass 590 nm filter. Images were processed and annotated using Adobe Photoshop 5.0.

Measurement of corticotropin secretion

Corticotropin secretion was measured essentially as described previously [12]. At 24 h after adenoviral infection, the culture medium was removed and the cells were washed twice with 2 ml of DMEM containing 0.1 % (w/v) BSA. To measure basal secretion, 1 ml of DMEM/BSA was added and the cells were incubated for 1 h at 37 °C. The medium was then centrifuged at 10000 *g* for 2 min at 4 °C. The supernatant (900 μl) was removed and stored at − 20 °C. Fresh DMEM/BSA (1 ml), containing 5 mM 8-Br-cAMP (8-bromo-cAMP), was then added to stimulate secretion. After a 1 h incubation at 37 °C, the medium was again centrifuged at 10000 *g* for 2 min, and 900 μl of supernatant was removed and stored at − 20 °C.

The corticotropin content of the cell supernatants was determined by RIA, based on the displacement of [3-^{125}I-iodotyrosyl-23]corticotropin (1–39; Amersham Biosciences) from a rabbit anti-human corticotropin antibody, essentially as described in [13]. Corticotropin standards were analysed in triplicate, and test samples in sextuplicate. Corticotropin released in 1 h of stimulated secretion was expressed as a percentage increase over that occurring during the 1 h period of basal secretion. Values are means ± S.E.M. Secretion from cells expressing the syncollin constructs was compared with that from control cells expressing GFP alone. The statistical significance of the differences was assessed by means of a Student's *t*-test for paired data.

Measurement of SEAP secretion

Cells were co-infected with adenoviruses encoding SEAP and appropriate syncollin or GFP construct, and incubated overnight at 37 °C. Cells were washed twice with 2 ml of DMEM containing 0.1 % BSA and then incubated in 1 ml of fresh DMEM containing 1 % BSA for 1 h at 37 °C. The medium was removed, stored on ice and replaced with 1 ml of fresh DMEM containing 1 % BSA and 5 mM 8-Br-cAMP. The cells were then incubated for a further 1 h at 37 °C. Samples of the medium were centrifuged at 420 *g* for 5 min at 4 °C, and supernatants were collected. The cells were washed twice in PBS (pH 7.4) and resuspended in DMEM containing 0.1 % (w/v) BSA and 0.2 % (v/v) Triton X-100. Samples were sonicated for 10 s and then centrifuged at 6800 *g* for 5 min at 4 °C. Again, samples of the supernatant were collected. SEAP activity was determined spectrophotometrically, using *p*-nitrophenyl phosphate as the substrate. SEAP activity was calculated from the slope of a plot of absorbance against time, and activity in the cell supernatants was expressed as a percentage of cell content under basal and stimulated conditions. Values are means ± S.E.M.

Electron microscopy

AtT-20 cells were removed from their culture flasks and rapidly concentrated by centrifugation. They were then re-suspended in fixative [4 % glutaraldehyde in 0.1 M Pipes buffer (pH 7.2) containing 2 mM $CaCl_2$] at 4 °C for 2 h, and embedded in Spurr's resin. Cell pellets were cut into thin sections (50 nm) and mounted on 300-mesh copper grids and stained with uranyl acetate followed by lead citrate. They were viewed with a Philips CM100 transmission electron microscope. Human erythrocytes (see below) were processed similarly.

Quantification of large, dense-core vesicles

Electron micrographs were taken of cells that had been infected with adenoviral constructs encoding GFP, syncollin or syncollin–GFP. Populations of large dense-core vesicles (diameter, 200 nm) were clearly visible in the processes of the cells. Vesicles within the tips of the processes were identified and counted. The total area of each tip was measured using ImageJ software, and the vesicle density for the tip (vesicles/μm^2) was calculated. Mean ± S.E.M. values of vesicle density over a number of tips were then determined. The numbers of juxtamembrane vesicles were also counted. Vesicles were placed in this category if any part of the vesicle lay within one vesicle diameter (i.e. 200 nm) of the plasma membrane. Values were expressed as number of vesicles/μm of membrane length (measured using ImageJ). Again, mean ± S.E.M. values over a number of tips were obtained. The statistical significance of differences was assessed by means of a Student's *t*-test for unpaired data.

Permeabilization of erythrocytes by syncollin

Human erythrocytes were collected and washed three times in HBS (Hepes-buffered saline, pH 7.6), containing 5 mM EGTA, 1 mg/ml BSA and protease inhibitor cocktail. The erythrocytes were then resuspended in 16 vol. of the same buffer without BSA. Erythrocyte suspensions (total volume, 100 μl) were incubated with various concentrations of rat pancreatic syncollin (added in taurodeoxycholate; final concentration, 0.05 %) for 90 min at 37 °C, with gentle mixing every 30 min. The erythrocytes were pelleted by centrifugation for 5 min at 21000 *g* and 4 °C. The absorbance of the supernatant was measured at 414 nm against a blank sample (containing incubation buffer only). Samples of erythrocytes were also incubated with 1 % Triton X-100 to determine the total amount of haemoglobin. Free haemoglobin was expressed as a percentage of the total. All measurements in each experiment were determined in triplicate. Values are means ± S.E.M.

Preparation of a crude membrane fraction from AtT-20 cells

Cells were detached from flasks and collected by centrifugation at 300 *g* for 3 min. After two washes in HBS, cells were incubated in hypotonic lysis buffer [10 mM Hepes (pH 7.6), 2 mM EDTA,

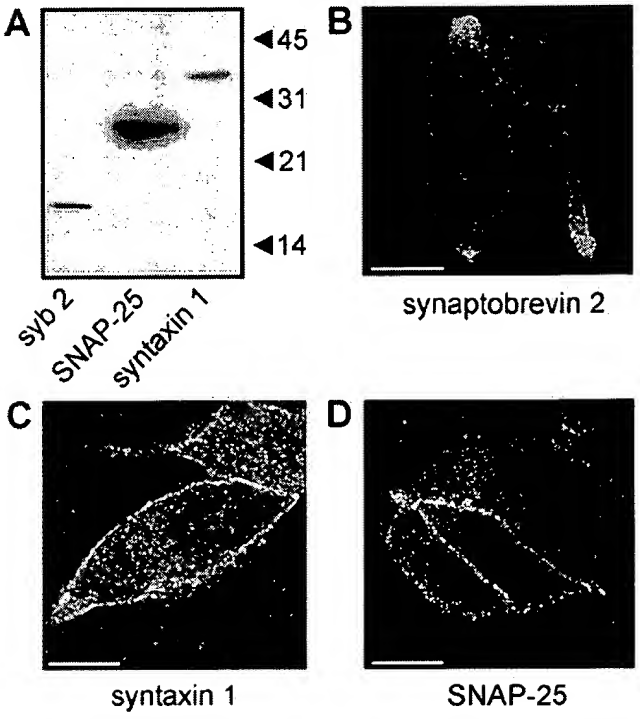

Figure 1 Expression of SNAREs in AtT-20 cells

(**A**) Immunoblot analysis of a membrane fraction from control cells. SNAREs were detected using mouse monoclonal antibodies to synaptobrevin 2 (syb2; 69.1; [27]), syntaxin (HPC-1; [28]) and SNAP-25 (71.1; [29]), all at 1:500 dilution, followed by HRP-conjugated anti-mouse secondary antibody (1:1000), with ECL® visualization. The positions of molecular-mass standards (kDa) are shown on the right. (**B–D**) Confocal immunofluorescence localization of synaptobrevin 2 (**B**), syntaxin 1 (**C**) and SNAP-25 (**D**). SNAREs were detected using the primary antibodies listed above (1:100), followed by either Cy3-conjugated (1:500; **B**) or FITC-conjugated (1:20; **C**, **D**) anti-mouse secondary antibodies. Scale bars, 10 μm.

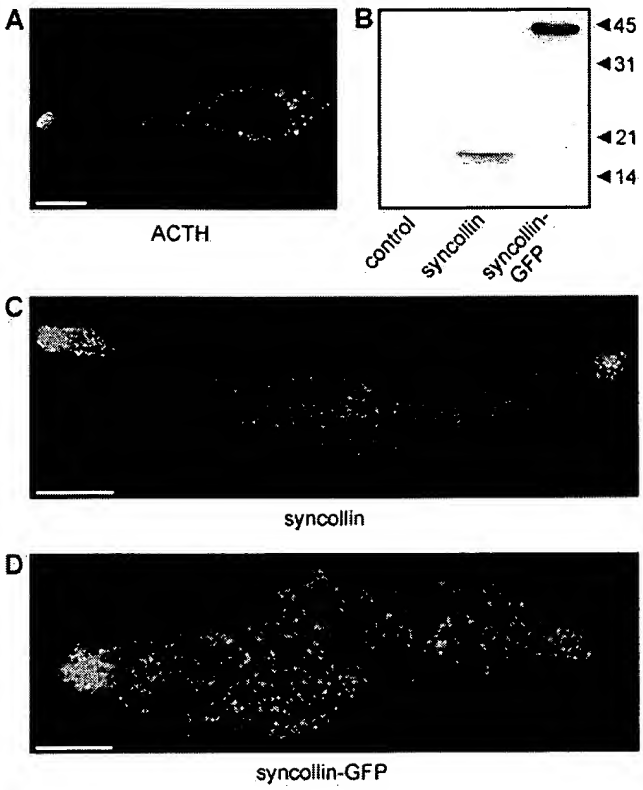

Figure 2 Expression of corticotropin and untagged and GFP-tagged syncollin in AtT-20 cells

(**A**) Confocal immunofluorescence localization of corticotropin. Corticotropin was detected using a rabbit polyclonal anti-corticotropin antibody (Sigma; 1:100), followed by an FITC-conjugated anti-rabbit secondary antibody (1:20). Scale bar, 10 μm. (**B**) Immunoblot analysis of crude cell extracts from control and adenovirally infected cells. Syncollin and syncollin–GFP were detected using mouse monoclonal anti-syncollin antibody 87.1 ([2]; 1: 500), followed by HRP-conjugated anti-mouse secondary antibody, with ECL® visualization. The positions of molecular-mass standards (kDa) are shown on the right. (**C**, **D**) Confocal immunofluorescence localization of syncollin (**C**) and syncollin–GFP (**D**) in adenovirally infected cells, using rabbit polyclonal anti-syncollin antibody 'B' ([15]; 1:100), followed by a TRITC-conjugated anti-rabbit secondary antibody (1:20). Scale bars, 10 μm.

1 mM PMSF and a protease inhibitor cocktail consisting of 1 μg/ml antipain, 50 μg/ml bacitracin, 1 μg/ml benzamidine, 1 μg/ml leupeptin, 1 μg/ml pepstatin and 10 μg/ml soybean trypsin inhibitor] for 20 min on ice. The cells were then homogenized with 30 strokes of a tight-fitting Dounce homogenizer. The homogenate was centrifuged at 400 *g* for 2 min at 4 °C to pellet cell debris. The supernatant was then centrifuged at 21 000 *g* for 15 min at 4 °C, and precipitated membranes were stored at − 80 °C until use.

RESULTS

The expression and distribution of SNAREs in AtT-20 cells, known to be involved elsewhere in exocytotic membrane fusion, were first established. Immunoblotting of a crude membrane fraction revealed the presence of the vesicle (v)-SNARE synaptobrevin 2 and the two target (t)-SNAREs syntaxin and SNAP-25 (synaptosome-associated protein of 25 kDa) (Figure 1A), in agreement with a previous report [14]. Immunofluorescence microscopy was then used to determine the intracellular localization of these proteins. Most of the adherent AtT-20 cells had one or more clearly recognizable processes. It was found that synaptobrevin was present mainly in a population of punctate structures at the tips of processes of the AtT-20 cells (Figure 1B). In contrast, syntaxin (Figure 1C) and SNAP-25 (Figure 1D) were both present throughout the plasma membrane.

The intracellular localization of corticotropin, the major peptide secreted by AtT-20 cells, was also established by immunofluorescence microscopy. As shown in Figure 2(A), corticotropin, like synaptobrevin 2, was found predominantly at the tips of the cell processes. To investigate the targeting of syncollin in AtT-20 cells, we infected them with adenoviruses expressing either untagged or GFP-tagged syncollin. Immunoblotting showed that syncollin was absent from uninfected cells, whereas bands of apparent molecular mass 16 and 45 kDa were detected in cells infected with virus encoding syncollin and syncollin–GFP, respectively (Figure 2B). The difference in size between the two proteins (29 kDa) corresponds to the known molecular mass of GFP. It should be noted that equal amounts of membranes were added to the syncollin and syncollin–GFP lanes in Figure 2(B). It was therefore possible to estimate by densitometric scanning of the blots that the relative expression levels of the two proteins were approx. 1:7 (syncollin/syncollin–GFP). This ratio was typical of the value obtained over a series of experiments. The intracellular distribution of untagged and GFP-tagged syncollin was investigated by immunofluorescence microscopy, using polyclonal anti-syncollin antibody 'B', the only antibody available to us that detects the

native protein [15]. As for synaptobrevin 2 and corticotropin, exogenous syncollin, both untagged (Figure 2C) and GFP-tagged (Figure 2D), was present in punctate structures predominantly located at the tips of cell processes.

It is known that neuroendocrine cells, such as neurons in the posterior pituitary [16] and pancreatic β-cells [17], possess both large dense-core vesicles and small 'synaptic-like' vesicles. It has also been shown previously that synaptobrevin is restricted to the membranes of small synaptic vesicles in rat brain [18]. Furthermore, other markers of the small synaptic-like vesicles, such as synaptophysin and synapsin I, are known to be absent from the membranes of the large dense-core vesicles in the posterior pituitary [16]. We were therefore interested in identifying the vesicle populations into which the proteins that were targeted to the tips of the cell processes (synaptobrevin 2, corticotropin and syncollin) were delivered. Double-label immunofluorescence microscopy revealed that syncollin and synaptobrevin 2 were not in fact co-localized, but were present in two distinct populations of vesicles (cf. green and red signals in Figure 3A). Corticotropin and synaptobrevin were also found to be differentially distributed (Figure 3B). Our results suggest that syncollin might be targeted to large dense-core vesicles, which contain corticotropin but not synaptobrevin 2, and excluded from small synaptic-like vesicles, which contain synaptobrevin 2 but not corticotropin. It was not possible to perform double-label (red/green) immunofluorescence microscopy for syncollin and corticotropin, first because the antibodies to the two proteins were both raised in rabbits, and secondly because the syncollin adenoviral construct also directs the expression of free GFP (to identify infected cells). We therefore compared the localization of GFP-tagged syncollin with that of corticotropin. As shown in Figure 3(C), the distribution of syncollin–GFP in the processes was almost identical with that of corticotropin. Hence, syncollin is efficiently targeted to corticotropin-positive vesicles in AtT-20 cells, as reported previously for syncollin expressed in these cells by transient transfection [15], but excluded from a separate population of vesicles containing synaptobrevin, which we suggest are small, synaptic-like vesicles. This finding, of course, leaves open the identity of the major v-SNARE in the secretory vesicle membrane. One candidate is cellubrevin, which has been shown to be present on dense-core vesicles in the anterior pituitary [14]. Figure 3(C) also reveals punctate structures in the body of the cell, which contain syncollin–GFP but not corticotropin. These may represent components of the secretory pathway (probably including the Golgi complex), which contain newly synthesized syncollin–GFP.

We next examined whether syncollin had any effect on the basal secretion of corticotropin from the AtT-20 cells. Basal corticotropin secretion was measured 24 h after infection, over a 1 h period, and corticotropin levels were determined by RIA. Basal secretion in cells expressing the syncollin constructs was expressed as a percentage of secretion in control cells (100%), infected with a GFP–adenovirus. The use of this control infection was important, because it has been reported previously that adenoviral infection of primary anterior pituitary cells can itself change the intracellular integrity of cells, and disrupt intracellular compartments, such as endosomes, as well as decreasing regulated secretion of corticotropin [19]. As illustrated in Figure 4(A), expression of either syncollin or syncollin–GFP had no effect on basal corticotropin secretion from the AtT-20 cells.

To investigate the effect of syncollin on constitutive secretion, AtT-20 cells were co-infected with adenoviruses encoding syncollin, syncollin–GFP or GFP, and a construct encoding SEAP, which is known to be secreted in a constitutive manner, e.g. in INS-1 cells, an insulin-secreting cell line [10]. After a 24 h adenoviral infection, the cells were incubated either under basal

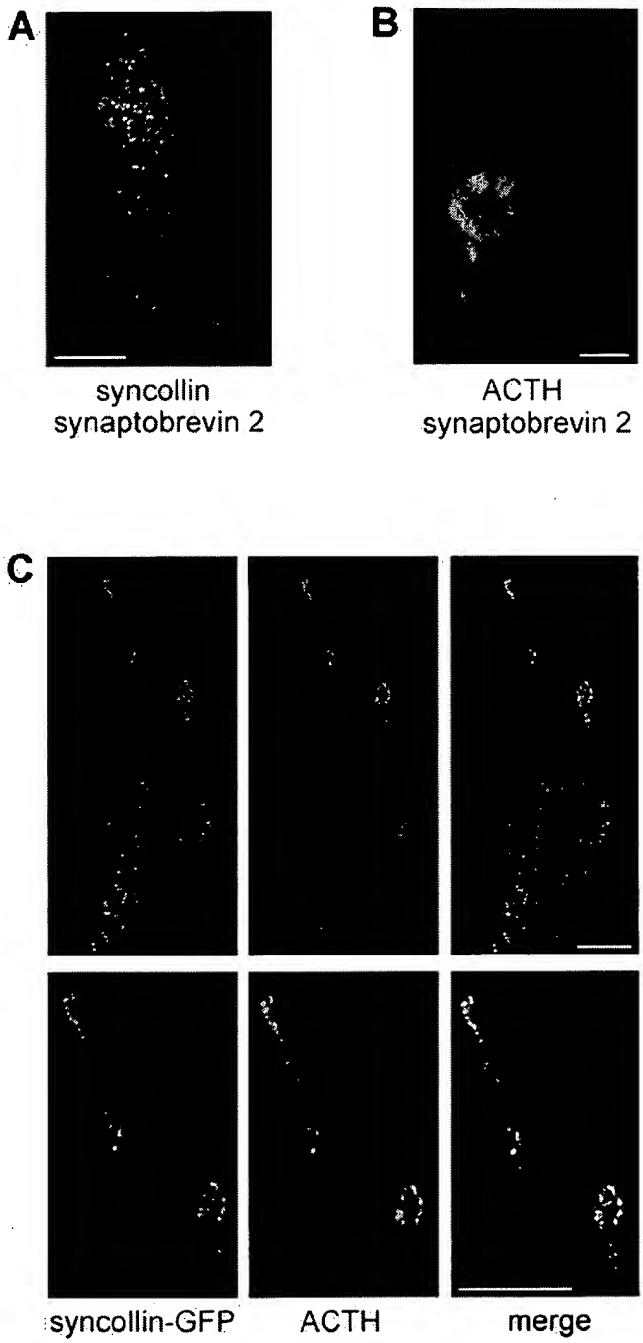

Figure 3 Protein targeting within the tips of AtT-20 cell processes

(**A**) Confocal immunofluorescence localization of syncollin and synaptobrevin 2. Syncollin was detected using rabbit polyclonal anti-syncollin antibody 'B' (1:100), followed by an FITC-conjugated anti-rabbit secondary antibody (1:20). Synaptobrevin was detected using mouse monoclonal anti-synaptobrevin antibody 69.1 (1:100), followed by a Cy3-conjugated anti-mouse secondary antibody (1:500). A cell process is shown at high magnification. Scale bar, 5 μm. (**B**) Localization of corticotropin and synaptobrevin 2. Corticotropin was detected using a rabbit polyclonal anti-corticotropin antibody (1:100), followed by an FITC-conjugated anti-rabbit secondary antibody (1:20). Synaptobrevin was detected using mouse monoclonal anti-synaptobrevin antibody 69.1 (1:100), followed by a Cy3-conjugated anti-mouse secondary antibody (1:500). A cell process is shown at high magnification. Scale bar, 2 μm. (**C**) Localization of syncollin–GFP and corticotropin. Syncollin–GFP was detected via its green fluorescence. Corticotropin was detected using a rabbit polyclonal anti-corticotropin antibody (1:100), followed by a TRITC-conjugated anti-rabbit secondary antibody (1:20). Upper panels: body of a cell, with two processes; lower panels: enlarged view of the tips of the processes. Scale bars, 10 μm.

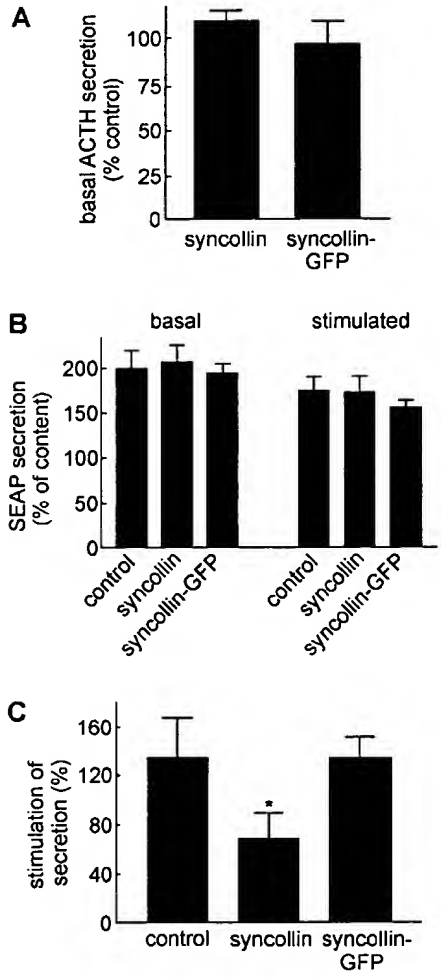

Figure 4 Effect of expression of syncollin and syncollin–GFP on secretion from AtT-20 cells

(**A**) Basal corticotropin secretion. Basal corticotropin secretion was measured 24 h after adenoviral infection over a 1 h period, and corticotropin levels were determined by RIA. Basal secretion in cells expressing the syncollin or syncollin–GFP constructs was expressed as percentage of secretion in cells expressing GFP ($n=7$). (**B**) Constitutive secretion of SEAP. Cells were co-infected with syncollin, syncollin–GFP or GFP (control), and a construct encoding SEAP. After a 24 h adenoviral infection, the cells were incubated either under basal conditions or in the presence of 8-Br-cAMP (5 mM). Supernatant and cells were harvested and the enzymic activity of SEAP in both fractions was measured. SEAP release was expressed as percentage of SEAP present in the cells ($n=7$). (**C**) Regulated secretion. Cells were infected with adenoviruses encoding syncollin, syncollin–GFP or GFP (control). After a 24-h infection period, the cells were incubated in serum-free medium, to determine the extent of basal corticotropin secretion, and then stimulated with 8-Br-cAMP (5 mM) to trigger regulated secretion. Corticotropin release was quantified by RIA, and the amount of corticotropin released after stimulation was expressed as a percentage increase in corticotropin secretion compared with basal secretion. (N.B. a 100% increase corresponds to a 2-fold stimulation). *$P < 0.05$ ($n=7$).

conditions or in the presence of 8-Br-cAMP (to induce a secretory response). Supernatant and cells were harvested and the enzymic activity of SEAP in both fractions was measured. SEAP release was expressed as a percentage of SEAP present in the cells. As shown in Figure 4(B), neither syncollin nor syncollin–GFP had any significant effect on SEAP release from the cells under either basal or stimulated conditions. Note that SEAP release was, if anything, reduced under conditions of stimulation, indicating that it does indeed represent constitutive secretion.

Regulated corticotropin secretion from adenovirus-infected cells expressing syncollin and syncollin–GFP was compared with secretion from cells infected with an adenovirus encoding GFP alone. After a 24 h infection period, the cells were incubated in the serum-free medium, to determine the extent of basal corticotropin secretion, and then stimulated with 8-Br-cAMP to trigger regulated secretion. The amount of corticotropin released after stimulation was expressed as a percentage increase in corticotropin secretion compared with basal secretion. As shown in Figure 4(C), syncollin lowered the regulated corticotropin secretion by about 50%, whereas syncollin–GFP, despite being expressed at an approx. 7-fold higher level, had no effect.

One possible explanation for the decrease in regulated secretion of corticotropin caused by syncollin expression is a reduction in vesicular corticotropin content. We attempted to determine the total cellular corticotropin content by RIA, and found that there was no discernible effect of syncollin. However, immunoblotting revealed that the antibody used in the RIA detected not only corticotropin but also the various precursor polypeptides (results not shown). Hence, the RIA provides little information about the levels of corticotropin itself. Furthermore, the corticotropin contained in the tips of the processes, where exocytosis occurs, probably represents a small fraction of total signal given by the cell lysates in the RIA.

It is also possible that the syncollin expression causes a decrease in secretory vesicle number. We tested this idea by counting the number of large dense-core vesicles at the tips of the processes of cells that had been infected with adenoviruses encoding syncollin, syncollin–GFP or GFP. The polarized structure of the cells was found to be preserved during the removal of the cells from their culture flasks, which involved firm tapping of the flasks to detach the cells followed by immediate fixation. The dense-core vesicles were easy to identify in electron micrographs of the cells (Figures 5A–5C). We counted both the total number of vesicles within the tips and the numbers of juxtamembrane vesicles [defined as those vesicles that were within one vesicle diameter (i.e. 200 nm) of the membrane]. We compared values obtained from cells expressing either syncollin–GFP or untagged syncollin with those for cells expressing GFP alone (control). We found that expression of syncollin–GFP had no significant effect either on the number of vesicles per unit area of cell process or on the number of juxtamembrane vesicles per unit length of membrane (Figures 5D and 5E). In contrast, expression of syncollin reduced the number of vesicles per unit area by 46%, relative to cells expressing GFP alone (Figure 5D), and reduced the number of juxtamembrane vesicles by 32% (Figure 5E). The fact that the reduction in vesicle numbers caused by syncollin was similar to the reduction in regulated corticotropin secretion strongly suggests that the two effects are causally connected.

How does syncollin affect the number of large, dense-core vesicles? In principle, it could be either decreasing vesicle biogenesis or destabilizing vesicles once they have been produced. The fact that syncollin is highly enriched in the vesicles themselves, rather than being concentrated on the secretory pathway, indicates that the latter is more probable. Furthermore, the lack of effect of syncollin on constitutive secretion (above) suggests that it is acting late in the secretory pathway. But does syncollin have any properties that might cause vesicle destabilization? We have reported recently that syncollin is able to permeabilize liposomes [3]. In the present study, we investigated this property in more detail by examining the effect of native syncollin, isolated from pancreatic zymogen vesicle membranes as described previously [2], on the integrity of human erythrocytes. Syncollin was solubilized in a small volume of 0.5% taurodeoxycholate and then diluted 10-fold into a suspension of erythrocytes. As shown in Figure 6(A),

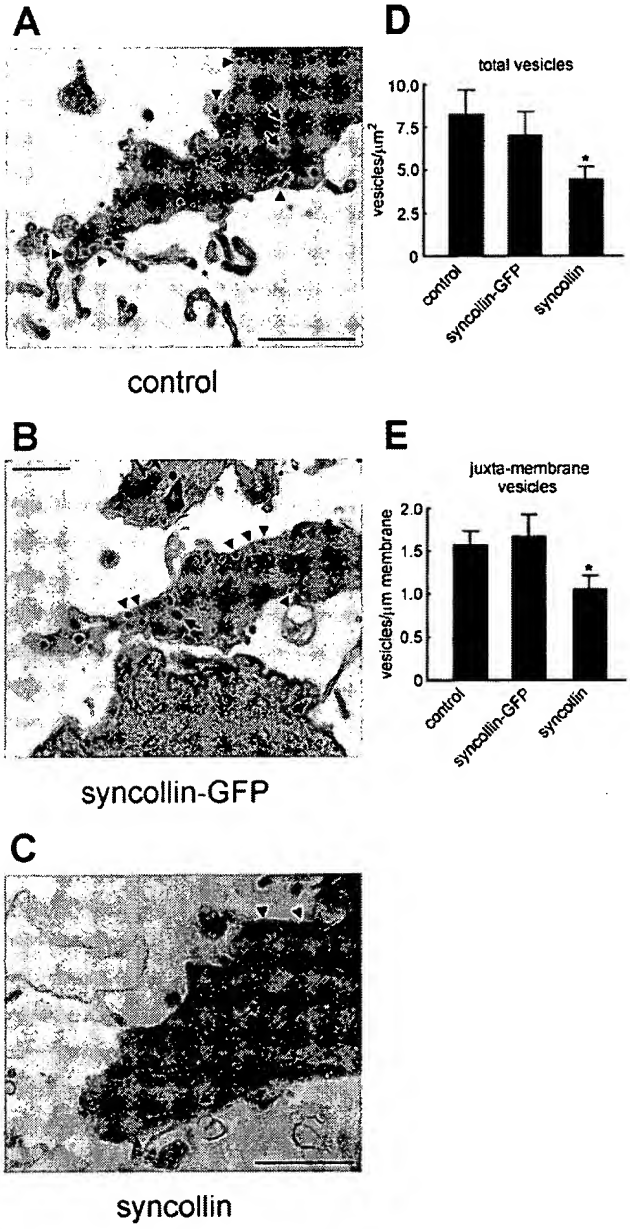

Figure 5 Effect of syncollin expression on large dense-core vesicle density at the tips of cell processes

(**A–C**) Electron micrographs showing the appearance of tips of the processes of cells infected with adenoviruses encoding GFP (**A**), syncollin–GFP (**B**) or syncollin (**C**). Arrowheads indicate large dense-core vesicles located within 200 nm of the plasma membrane; arrows indicate vesicles deeper within the tip. Scale bars, 2 μm (**A**), 1 μm (**B**, **C**). (**D**) Mean total vesicle density within the tips of the processes. For cells expressing GFP (control), 19 processes were analysed, which contained a total of 590 vesicles; for cells expressing syncollin–GFP, 20 processes were found to contain a total of 691 vesicles; for cells expressing syncollin, 20 processes contained a total of 379 vesicles. *$P < 0.05$ relative to control. (**E**) Mean number of juxtamembrane vesicles in the cell processes [defined as those vesicles lying within one vesicle diameter (i.e. 200 nm) of the plasma membrane]. The total numbers of juxtamembrane vesicles were GFP (control), 313 vesicles; syncollin–GFP, 372 vesicles; syncollin, 229 vesicles. *$P < 0.05$, relative to control.

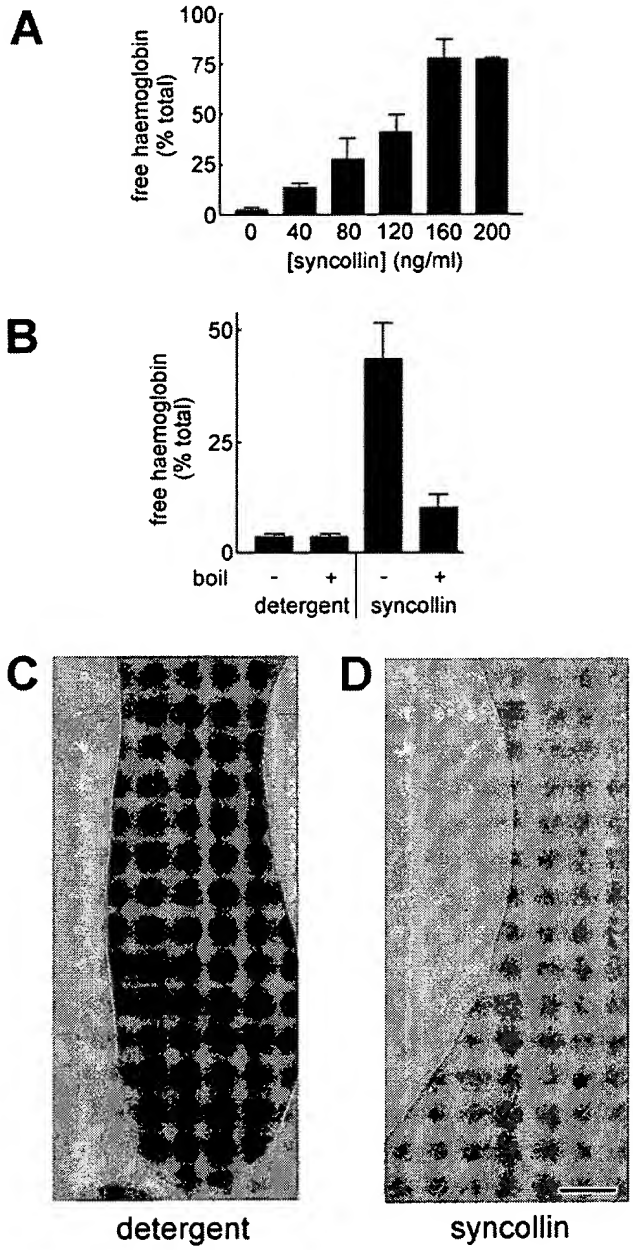

Figure 6 Purified syncollin permeabilizes erythrocytes

(**A**) Concentration dependence of the effect of syncollin. Erythrocyte suspensions (total volume, 100 μl) were incubated with various concentrations of syncollin (added in taurodeoxycholate; final concentration 0.05 % in all samples) for 90 min at 37 °C. The erythrocytes were pelleted by centrifugation, and the absorbance of the supernatant was measured at 414 nm. Samples of erythrocytes were also incubated with 1 % Triton X-100 to determine the total amount of haemoglobin. Free haemoglobin was expressed as a percentage of the total. All points in each experiment were determined in triplicate ($n = 3$ experiments). (**B**) Effect of boiling on the ability of syncollin and detergent to permeabilize erythrocytes. Erythrocyte suspensions were incubated with either taurodeoxycholate (0.05 %) or syncollin (120 ng/ml), either untreated or boiled for 30 min, for 90 min at 37 °C, and the percentage of haemoglobin released into the supernatant was determined ($n = 4$). Electron micrographs of sections through erythrocytes treated with either (**C**) taurodeoxycholate (0.05 %) or (**D**) syncollin (120 mg/ml). Note that the membranes of both cells are apparently intact, and that the content of the syncollin-treated cell is less electron dense than that of the detergent-treated cell. Scale bar, 100 nm.

syncollin produced a significant, concentration-dependent permeabilization of the erythrocytes, as measured by the release of haemoglobin into the surrounding solution. Taurodeoxycholate alone, at a final concentration of 0.05 %, produced a very low level of permeabilization. Figure 6(B) shows that, as expected from a protein-mediated effect, the ability of syncollin to permeabilize erythrocytes was almost abolished after boiling for 30 min. The

small effect of taurodeoxycholate alone was unaffected by similar treatment. To ascertain whether syncollin was causing haemoglobin release through a gross lytic effect on the erythrocytes, cells that had been incubated with either detergent (0.05%) or syncollin (120 ng/ml) for 90 min were examined by electron microscopy. The images in Figure 6(C) are typical of a number of sections taken through the two populations of erythrocytes. It can be seen that both detergent- and syncollin-treated cells have apparently intact membranes; however, the content of the syncollin-treated erythrocyte is considerably less electron-dense than that of the detergent-treated cell, as expected from the observed haemoglobin release. If syncollin also has a membrane-permeabilizing effect from within the large, dense-core vesicles in AtT-20 cells, then this would account for the observed reduction in vesicle numbers.

Why does untagged syncollin inhibit regulated corticotropin release, whereas GFP-tagged syncollin has no effect? The GFP tag added to syncollin to produce syncollin–GFP is approx. twice as large as syncollin itself. It is highly probable, therefore, that the structure and properties of syncollin will be profoundly altered by the presence of the tag. This in turn could account for the effect on regulated secretion of untagged, but not tagged, syncollin. In an attempt to identify the crucial difference between syncollin and syncollin–GFP, membrane fractions from adenovirally infected cells were prepared and the behaviour of the two proteins was further studied. Both proteins were found in the membrane fractions under normal conditions, but both were completely removed from the membranes by treatment with 0.1 M sodium carbonate (pH 11.0; Figure 7A). This behaviour is identical with that of native syncollin present in zymogen vesicles [2].

Pancreatic syncollin interacts with cholesterol in the inner leaflet of zymogen granule membranes [4]. Consistent with this, native syncollin can be co-immunoprecipitated with cholesterol and is partially removed from zymogen granule membranes by incubation with MβCD (methyl-β-cyclodextrin), a cholesterol-depleting agent [4]. This effect is enhanced by additional treatment with KCl. To study the interactions of syncollin and syncollin–GFP expressed in AtT-20 cells with cholesterol, similar experiments were performed with membranes prepared from adenovirally infected cells. Membranes were incubated overnight in buffer (HBS), KCl (200 mM), MβCD (50 mg/ml), or MβCD plus KCl. Membranes and supernatant were then separated by centrifugation and the distribution of syncollin between the fractions was analysed. As illustrated in Figure 7(B), about half of the untagged syncollin was removed from the membrane during incubation in the buffer. Syncollin was completely removed with KCl and with KCl plus MβCD; with MβCD alone about two-thirds was removed. In contrast, syncollin–GFP remained completely bound to the membrane in the buffer. About half was removed with KCl, and about one-third with MβCD. Even during incubation with MβCD plus KCl, only approx. two-thirds of the syncollin–GFP was removed from the membrane. This result demonstrates that syncollin–GFP is more tightly attached to AtT-20 cell membranes compared with untagged syncollin. In contrast with the behaviour of syncollin and syncollin–GFP, SNAP-25 (which is known to be anchored to membranes via palmitoyl residues [20]) remained bound to the membranes during all treatments.

As described above, native pancreatic syncollin exists in a homo-oligomeric form, and the component monomers can be irreversibly cross-linked by various chemical reagents, such as bis(sulphosuccinimidyl)suberate (BS^3; [2]). To determine whether syncollin and syncollin–GFP expressed in the AtT-20 cells also formed homo-oligomers, we performed BS^3 cross-linking experiments with membranes from adenovirally infected cells. As

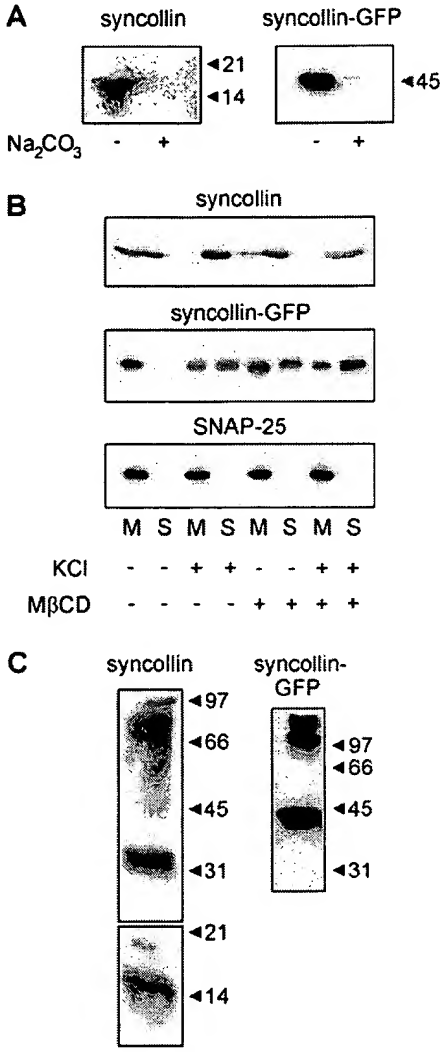

Figure 7 Biochemical characteristics of syncollin and syncollin–GFP expressed in AtT-20 cells

(**A**) Effect of carbonate washing on the membrane association of syncollin and syncollin–GFP. Cells were infected with adenoviruses encoding either syncollin or syncollin–GFP, and membrane fractions were prepared from them 24 h later. The membranes were incubated either in HBS or in Na_2CO_3 (100 mM; pH 11.0) for 30 min at 4 °C. Membranes were then pelleted by centrifugation, and the presence of syncollin was determined by immunoblotting, using mouse monoclonal anti-syncollin antibody 87.1 (1:500), followed by HRP-conjugated anti-mouse secondary antibody (1:1000), with ECL® visualization. The positions of molecular-mass standards (kDa) are shown on the right. (**B**) Effect of KCl washing and cholesterol depletion on the membrane association of syncollin and syncollin–GFP. Membranes prepared from adenovirally infected cells were incubated at 4 °C overnight in HBS, KCl (200 mM), MβCD (50 mg/ml) or KCl plus MβCD. Membranes were then pelleted by centrifugation and equivalent fractions of membranes (M) and supernatant (S) were analysed by immunoblotting, using mouse monoclonal anti-syncollin antibody 87.1 and mouse monoclonal anti-SNAP-25 antibody 71.1. (**C**) Cross-linking of membrane-associated syncollin and syncollin–GFP. Membranes prepared from adenovirally infected cells were solubilized in 0.5% taurodeoxycholate and incubated with the cross-linker BS^3 (4 mM) for 30 min at 4 °C. Samples were then analysed by immunoblotting, using mouse monoclonal anti-syncollin antibody 87.1. Positions of molecular-mass standards (kDa) are shown on the right.

shown in Figure 7(C), both syncollin and syncollin–GFP formed higher-order structures. Because of the relatively low level of expression of untagged syncollin, only weak signals were detected for higher-order bands. However, one prominent band was detected at 32 kDa, which quite probably represents a dimer. Further

higher bands could represent homo-oligomers up to hexamers. A band at 21 kDa was also detected; this was seen previously in cross-linking experiments with pancreatic zymogen granule membranes [2,3]. At present, we are uncertain as to what this band represents. Cross-linked syncollin–GFP gave a band at 45 kDa, corresponding to the monomer, and another at approx. 97 kDa, which quite probably represents the dimer. At least one band with a higher molecular mass was detected, which could represent a higher-order form of syncollin–GFP. For both syncollin and syncollin–GFP, no higher molecular-mass bands were detected after incubation with pre-quenched cross-linker (results not shown). This experiment suggests that both syncollin and syncollin–GFP form homo-oligomers in AtT-20 cells. It should be noted, however, that GFP has been shown to homo-oligomerize on the secretory pathway in AtT-20 cells [21], most probably through the formation of intermolecular disulphide bonds. Hence, we cannot exclude the possibility that homo-oligomerization of syncollin–GFP is mediated by its GFP tag rather than syncollin itself.

DISCUSSION

We have shown here that syncollin, expressed exogenously in AtT-20 cells, is delivered to a population of secretory vesicles that contain corticotropin but not the v-SNARE synaptobrevin 2. Once present in the dense-core vesicles at the tips of the AtT-20 cell processes, syncollin brings about a 2-fold reduction in the numbers of vesicles, accompanied by a 2-fold reduction of regulated corticotropin secretion. We did not find any effect of syncollin expression on the total cellular levels of corticotropin or its precursor polypeptides (results not shown). Further, in a parallel study on pancreatic β-cells, we again found that syncollin expression reduced regulated insulin secretion without any effect on pro-insulin synthesis or insulin gene expression (L. B. Hays, B. Wicksteed, Y. Wang, J. F. McCuaig, P. A. Halban, L. H. Philipson, J. M. Edwardson and C. J. Rhodes, unpublished work). In addition, although the corticotropin-containing vesicles are reduced in number, they are still correctly targeted to the tips of the AtT-20 cell processes in the presence of syncollin (results not shown). All of these lines of evidence point to an effect of syncollin late in the secretory pathway, consistent with the concentration of syncollin in vesicles at the tips of the cell processes.

The physiological role of syncollin has been addressed recently in a study of the phenotype of syncollin-deficient mice [7]. Abnormalities in pancreatic function in the syncollin knockout mice were observed; for instance, the necrotic response to hyper-stimulation with caerulein was shown to be more severe in the knockout mice than in wild-type mice. Furthermore, both the rate of synthesis of new proteins and the rate at which they are released from the pancreatic lobules under conditions of stimulation were decreased. However, tissue amylase levels were reported to be unchanged, and there was no reduction in the rate of secretion of pre-formed amylase. Since the final secretory step appeared to be normal, whereas the rate of delivery of newly synthesized protein to the late stages of the secretory pathway was decreased, it was suggested that syncollin might play a role in the packaging of proteins into the zymogen granules [7]. We have recently performed our own analysis of the phenotype of the syncollin knockout mice (B. Wäsle, M. Turvey, O. Larina, P. Thorn, J. Skepper, A. J. Morton and J. M. Edwardson, unpublished work). In contrast with the results reported previously, we have found that these mice have pancreatic hypertrophy and increased pancreatic amylase levels. Secretagogue-stimulated amylase release from pancreatic lobules of syncollin knockout mice was reduced by about 50 % compared with wild-type lobules, and the number of individual exocytotic events in response to secretagogue stimulation was reduced by the same factor. Furthermore, the delivery of newly synthesized protein to zymogen granules was delayed, indicating a 'backing-up' effect on the secretory pathway. Although we can offer no explanation for the differences between our results and those reported previously, we would argue that our findings strongly indicate that syncollin plays a significant role in exocytosis in the pancreatic acinar cell.

We have reported that syncollin exists as a doughnut-shaped homo-oligomer with a 5 nm central hole [3]. This structure, together with evidence that syncollin can permeabilize liposomes [3], indicates that the protein might have pore-forming properties. The ability of syncollin to render erythrocytes leaky to haemoglobin, a protein of molecular diameter 5 nm, without causing gross lysis of the cells, is consistent with the notion that it can form pores in membranes. Syncollin might therefore cause the uncontrolled generation of pores in the membranes of the vesicles in the AtT-20 cells. The vesicles that have been 'holed' through the action of syncollin might then be rapidly cleared from the cell. In this way, the vesicle population at steady state would consist of fewer intact vesicles rather than the same number of vesicles each containing less corticotropin.

In the pancreatic acinar cell, the presence of doughnut-shaped structures in the zymogen granule membrane visualized by freeze-fracture electron microscopy was reported a number of years ago [22]. Furthermore, it is known that cholesterol is switched from the cytoplasmic leaflet of the granule membrane to the luminal leaflet as the granules mature [23], a change that would favour the insertion of syncollin, a cholesterol-binding protein [4], into the membrane of the maturing zymogen granule. (Note also that cholesterol represents 23 % of the lipid composition of human erythrocyte membranes [24].) Although evidence has been presented previously that digestive enzymes are able to leak out of isolated zymogen granules [25], through pores of effective diameter 5 nm [26], the apparent stability of the granule population within the acinar cell indicates that the granules are unlikely to contain pores that are constitutively active. If this is the case, then the pore-forming property of syncollin must normally be under inhibitory control, perhaps through the interaction of syncollin with another protein. If its ability to form pores is its key property, it is possible that, in response to some unidentified trigger, it is able to penetrate the zymogen granule membrane at the point of fusion between the granule and the plasma membrane and contribute to the formation of the fusion pore.

Results of the present study show that the addition of a GFP tag to syncollin completely abolishes its ability to perturb the later stages of the secretory pathway in AtT-20 cells. Although the membrane association of syncollin–GFP is slightly tighter than that of untagged syncollin, we have not been able to identify any gross biochemical differences between the two forms of the protein that might account for the significant difference in their functional effects. Both untagged and tagged syncollin, for example, are able to form homo-oligomers. It is probable, therefore, that the presence of the GFP tag (which is twice as large as syncollin itself) has a significant effect on the structure of the syncollin homo-oligomer that might, for example, interfere with its ability to form pores in the membrane. It should be pointed out that the ability of syncollin–GFP to become targeted faithfully to secretory vesicles in 'foreign' cells, combined with its lack of effect on the secretory process, makes it an ideal marker for the visualization of exocytosis in cells containing large, dense-core vesicles.

We thank R. Jahn (Max-Planck Institute for Biophysical Chemistry, Göttingen, Germany) for providing antibodies, P. A. Halban (University of Geneva, Switzerland) for the SEAP-adenovirus, S. Guild (School of Biology, University of St. Andrews, U.K.) for advice

regarding the assay for corticotropin secretion, and J. Skepper (Multi-Imaging Laboratory, Department of Anatomy, University of Cambridge, U.K.) for expert assistance with the electron microscopy. This work was supported by Project Grant 063920 from the Wellcome Trust (to J. M. E.) and Grant DK47919 from the NIH (to C. J. R.).

REFERENCES

1 Edwardson, J. M., An, S. and Jahn, R. (1997) The secretory granule protein syncollin binds to syntaxin in a Ca^{2+}-sensitive manner. Cell (Cambridge, Mass.) **90**, 325–333
2 An, S. J., Hansen, N. J., Hodel, A., Jahn, R. and Edwardson, J. M. (2000) Analysis of the association of syncollin with the membrane of the pancreatic zymogen granule. J. Biol. Chem. **275**, 11306–11311
3 Geisse, N. A., Wäsle, B., Saslowsky, D. E., Henderson, R. M. and Edwardson, J. M. (2002) Syncollin homo-oligomers associate with lipid bilayers in the form of doughnut-shaped structures. J. Membr. Biol. **89**, 83–92
4 Hodel, A., An, S. J., Hansen, N. J., Lawrence, J., Wäsle, B., Schrader, M. and Edwardson, J. M. (2001) Cholesterol-dependent interaction of syncollin with the membrane of the pancreatic zymogen granule. Biochem. J. **356**, 843–850
5 Kalus, I., Hodel, A., Koch, A., Kleene, R., Edwardson, J. M. and Schrader, M. (2002) Interaction of syncollin with GP-2, the major membrane protein of pancreatic zymogen vesicles, and association with lipid microdomains. Biochem. J. **362**, 433–442
6 Tan, S. and Hooi, S. C. (2000) Syncollin is differentially expressed in rat proximal small intestine and regulated by feeding behaviour. Am. J. Physiol. **278**, G308–G320
7 Antonin, W., Wagner, M., Riedel, D., Brose, N. and Jahn, R. (2002) Loss of the zymogen granule protein syncollin affects pancreatic synthesis and transport but not secretion. Moll. Cell. Biol. **22**, 1545–1554
8 He, T. C., Zhou, S., da Costa, L. T., Yu, J., Kinzler, K. W. and Vogelstein, B. (1998) A simplified system for generating recombinant adenoviruses. Proc. Natl. Acad. Sci. U.S.A. **95**, 2509–2514
9 Dickson, L. M., Lingohr, M. K., McCuag, J., Hugl, S. R., Snow, L., Kahn, B. B., Myers, Jr, M. G. and Rhodes, C. J. (2001) Differential activation of protein kinase B and p70(S6)K by glucose and insulin-like growth factor 1 in pancreatic β-cells (INS-1). J. Biol. Chem **276**, 21110–21120
10 Molinete, M., Lilla, V., Jain, R., Joyce, P. B., Gorr, S. U., Ravazzola, M. and Halban, P. A. (2000) Trafficking of non-regulated secretory proteins in insulin secreting (INS-1) cells. Diabetologia **43**, 1157–1164
11 Madziva, M. T. and Edwardson, J. M. (2001) Trafficking of green fluorescent protein-tagged muscarinic M_4 receptors in NG108-15 cells. Eur. J. Pharmacol. **428**, 9–18
12 McFerran, B. W. and Guild, S. B. (1994) Effects of protein kinase C activators upon the late stages of the ACTH secretory pathway of AtT-20 cells. Br. J. Pharmacol. **113**, 171–178
13 McFerran, B. W. and Guild, S. B. (1995) Effects of mastoparan upon the late stages of the ACTH secretory pathway of AtT-20 cells. Br. J. Pharmacol. **115**, 696–702
14 Majó, G., Aguado, F., Blasi, J. and Marsal, J. (1998) Synaptobrevin isoforms in secretory vesicles and synaptic-like microvesicles in anterior pituitary cells. Life Sci. **62**, 607–616
15 Hodel, A. and Edwardson, J. M. (2000) Targeting of the zymogen-granule protein syncollin in AR42J and AtT-20 cells. Biochem. J. **350**, 637–643
16 Navone, F., Di Gioia, G., Jahn, R., Browning, M., Greengard, P. and De Camilli, P. (1989) Microvesicles of the neurohypophysis are biochemically related to small synaptic vesicles of presynaptic nerve terminals. J. Cell Biol. **109**, 3425–3433
17 Reetz, A., Solimena, M., Matteoli, M., Folli, F., Takei, K. and De Camilli, P. (1991) GABA and pancreatic β-cells: colocalization of glutamic acid decarboxylase (GAD) and GABA with synaptic-like microvesicles suggests their role in GABA storage and secretion. EMBO J. **10**, 1275–1284
18 Baumert, M., Maycox, P. R., Navone, F., De Camilli, P. and Jahn, R. (1989) Synaptobrevin: an integral membrane protein of 18 000 daltons present in small synaptic vesicles of rat brain. EMBO J. **8**, 379–384
19 Castro, M. G., Goya, R. G., Sosa, Y. E., Rowe, J., Larregina, A., Morelli, A. and Lowenstein, P. R. (1997) Expression of transgenes in normal and neoplastic anterior pituitary cells using recombinant adenoviruses: long term expression, cell cycle dependency, and effects on hormone secertion. Endocrinology **138**, 2184–2194
20 Hess, D. T., Slater, T. M., Wilson, M. C. and Skene, J. H. (1992) The 25 kDa synaptosomal-associated protein SNAP-25 is the major methionine-rich polypeptide in rapid axonal transport and a major substrate for palmitoylation in adult CNS. J. Neurosci. **12**, 4634–4641
21 Jain, R. K., Joyce, P. B., Molinete, M., Halban, P. A. and Gorr, S. U. (2001) Oligomerization of green fluorescent protein in the secretory pathway of endocrine cells. Biochem. J. **360**, 645–649
22 Cabana, C., Magny, P., Nadeau, D., Grondin, G. and Beaudoin, A. (1987) Freeze-fracture study of the zymogen granule membrane of pancreas: two novel types of intramembrane particles. Eur. J. Cell Biol. **45**, 246–255
23 Orci, L., Miller, R. G., Montesano, R., Perrelet, A., Amherdt, M. and Vassalli, P. (1980) Opposite polarity of filipin-induced deformations in the membrane of condensing vacuoles and zymogen granules. Science **210**, 1019–1021
24 Hertle, R. (2002) *Serratia marcescens* hemolysin (ShlA) binds artificial membranes and forms pores in a receptor-independent manner. J. Membr. Biol. **189**, 1–14
25 Goncz, K. K. and Rothman, S. (1992) Protein flux across the membrane of single secretion granules. Biochim. Biophys. Acta **1109**, 7–16
26 Goncz, K. K. and Rothman, S. (1992) A trans-membrane pore can account for protein movement across zymogen granule membranes. Biochim. Biophys. Acta **1238**, 91–93
27 Edelmann, L., Hanson, P. I., Chapman, E. R. and Jahn, R. (1995) Synaptobrevin binding to synaptophysin: a potential mechanism for controlling the exocytotic membrane fusion machine. EMBO J. **14**, 224–231
28 Barnstable, C. J., Hofstein, R. and Akagawa, K. (1985) A marker of early amacrine cell development in rat retina. Dev. Brain Res. **20**, 286–290
29 Xu, T., Rammner, B., Margittai, M., Artalejo, A. R., Neher, E. and Jahn, R. (1999) Inhibition of SNARE complex assembly differentially affects kinetic components of exocytosis. Cell (Cambridge, Mass.) **99**, 713–722

Received 13 November 2003/23 March 2004; accepted 24 March 2004
Published as BJ Immediate Publication 24 March 2004, DOI 10.1042/BJ20031726